Manganese Substantially Alters the Dynamics of Translesion DNA Synthesis†

Heather Hays‡ and Anthony J. Berdis*,§

Department of Chemistry, Case Western Reserve University, 2109 Adelbert Road, Cleveland, Ohio 44106, and The Comprehensive Cancer Center and Department of Pharmacology, School of Medicine, Case Western Reserve University, 10900 Euclid Avenue, Cleveland, Ohio 44106

Received November 16, 2001; Revised Manuscript Received January 29, 2002

ABSTRACT: The effect of metal ion substitution on the dynamics of translesion DNA synthesis catalyzed by the bacteriophage T4 DNA polymerase was quantitatively evaluated through steady-state and transient kinetic techniques. Substitution of Mn^{2+} for Mg^{2+} enhances the steady-state rate of dNMP misinsertion opposite an abasic site by 11−34-fold. At the molecular level, the enhancement in translesion DNA synthesis reflects a substantial increase in the rate of the conformational change preceding phosphoryl transfer for all dNTPs that were tested. This is best illustrated by the biphasic pre-steady-state time course of dAMP insertion opposite an abasic site which indicates that a step after chemistry is rate-limiting for steady-state enzyme turnover. Furthermore, the k_{pol} value of 40 s^{-1} measured under single-turnover reaction conditions is 20-fold greater than the k_{cat} value of 2 s^{-1} measured for steady-state enzyme turnover. Finally, the low elemental effect (∼2.4-fold reduction in k_{pol}) measured by substituting the α-thiotriphosphate analogue for dATP further argues that chemistry is not rate-limiting. In contrast to the biphasic insertion of dAMP, pre-steady-state time courses for the insertion of dCMP, dGMP, or dTMP opposite an abasic site were linear. Nearly identical k_{pol} values (∼1 s^{-1}) were measured for the insertion of dCMP, dGMP, and dTMP opposite the abasic site using single-turnover conditions. However, the large elemental effects of 27 and 70 measured by substituting the α-thiotriphosphate analogues for dCTP and dGTP, respectively, suggest that phosphoryl transfer may be the rate-limiting step for their insertion opposite the abasic site. Various models are discussed in an attempt to explain the effect of metal ion substitution on the dynamics of translesion DNA replication.

DNA polymerases catalyze the rapid incorporation of dNMPs across from a DNA template. These enzymes typically maintain a remarkable degree of substrate specificity despite the fact that dNMP incorporation changes during each cycle of nucleotide addition as directed by the sequence of the DNA template. The extraordinary fidelity of DNA replication is accomplished through at least two distinct enzymatic reactions. The first encompasses selective incorporation of the correctly base-paired nucleotide, while the second involves removal of mismatched bases by the 3′ → 5′ exonuclease proofreading ability of the enzyme. These two enzymatic activities provide an error rate of one misincorporation event per 10^8 base pairs.

However, cellular exposure to exogenous and endogenous sources of reactive chemicals and oxygen species leads to the formation of DNA adducts (*1*, *2*) which are potentially miscoding and precursors to mutagenic events if replicated by DNA polymerases (*3*). The miscoding potential of DNA adducts results from the ability of the adduct to form incorrect base pairs which may escape editing by the polymerase and/or repair by various DNA repair systems (*4*). Perhaps the most prevalent and damaging DNA adduct is an apurinic/apyrimidinic (abasic)[1] site which can arise spontaneously under normal physiological conditions (*5*) as well as through the action of base excision repair pathways (*6*). This DNA lesion lacks potential hydrogen bonding capabilities and thus presents the opportunity for the DNA replicase to incorporate any of the four nucleosides, thereby enhancing the potential to create a genetic mutation.

One key step in preventing the establishment and propagation of mutagenic events is the high degree of fidelity of the DNA polymerase maintained during replication. The central dogma of DNA replication is that the extraordinary efficiency and fidelity of the DNA polymerase are dictated by the hydrogen bonds formed between the template nucleobases with incoming nucleoside triphosphates. While Watson−Crick hydrogen bonds provide a stabilizing effect on nucleic acid structure, it has been recently demonstrated that hydrogen bonding is not an absolute requirement for DNA polymerization activity (*7*−*11*). For example, Kool et al. (*7*) have demonstrated that difluorotoluene deoxynucleoside, a nonpolar mimic of thymidine, is efficiently inserted opposite adenine. The same group has demonstrated that dPTP, a nucleoside triphosphate with pyrene replacing the normal

† This research was supported through funding from the Steris Foundation and the American Cancer Society (IRG-91-022-06-IRG) to The Comprehensive Cancer Center at Case Western Reserve University and University Hospitals of Cleveland.

* To whom correspondence should be addressed. Telephone: (216) 368-6255. Fax: (216) 368-3395. E-mail: ajb15@po.cwru.edu.

‡ Department of Chemistry.

§ School of Medicine.

[1] Abbreviations: abasic, apurinic/apyrimidinic; TBE, Tris-HCl, borate, and EDTA; EDTA, ethylenediaminetetraacetate, sodium salt; dNTP, deoxynucleoside triphosphate; α-S-dNTP, deoxynucleoside 5′-*O*-(3-thiotriphosphate).

10.1021/bi0120648 CCC: $22.00
Published on Web 03/22/2002

purine or pyrimidine nucleobase, is likewise incorporated across from an abasic site (*9*). Furthermore, our own studies have demonstrated that the bacteriophage T4 DNA polymerase is capable of preferential insertion of dAMP across from an abasic site (*11*). Through a series of steady-state and transient kinetic experiments, we further demonstrated that the rate-limiting step for insertion across from an abasic site is the conformational change preceding phosphoryl transfer (*11*). Although the same kinetic step is also rate-limiting during precise DNA replication, the rate of the conformational change is reduced 660-fold in the former case when compared to the latter. Surprisingly, the rate of the conformational change during translesion DNA synthesis was dependent upon the nucleoside being inserted such that the rate is further reduced between 4000- and 17000-fold during incorporation of the other dNMPs. These data collectively demonstrate that the lack of hydrogen bonding does not prevent DNA replication but instead lowers the efficiency of nucleotide insertion.

These observations beg the fundamental question regarding the efficacy of DNA replication; i.e., what truly dictates the high degree of fidelity during DNA polymerization if hydrogen bonds are not essential for efficient DNA replication? One reasonable answer is provided by the "induced fit" model for the maintenance of fidelity. The induced fit model is generally viewed as a substrate selection gate by which initial "loose" binding of the correct substrate triggers a conformational change that leads to an active configuration of the enzyme (*12*). In this active configuration, transition-state stabilization for catalysis is provided when key active site residues are brought into proper alignment. In most instances, the binding of an incorrect dNTP causes an inappropriate fit by disturbing precise geometry needed for proper alignment of the incoming nucleobase with the template. The net result is that the conformational change preceding phosphoryl transfer occurs at a slower rate to substantially retard nucleoside insertion. At the molecular level, this mode of inappropriate dNTP binding is presumed to reflect perturbations in the proper hydrogen bonding network normally observed during correct nucleoside triphosphate insertion. However, the differences in free energy caused by formation of improper hydrogen bonds (~0.2−4.0 kcal/mol) (*13*−*15*) cannot entirely account for the high degree of fidelity. Thus, alternative or augmenting models must be invoked. Our previously published kinetic data revealed a distinctive correlation between the efficiency of nucleoside insertion (*11*) with the potential for the nucleobase to be in an intrahelical versus extrahelical configuration (*16*). The nucleotide dependency on the rate of the conformational change suggests that the dynamics of nucleotide insertion across from and beyond the abasic site are not dictated by hydrogen bonding potential but instead are predominantly controlled by the relative configuration of the formed dNMP−abasic site mispair. Our data, in conjunction with the demonstration of efficient insertion of nonpolar nucleoside analogues (*7*−*10*), suggest that base stacking may compensate for the lack of proper hydrogen bond formation in playing a large role in aiding the polymerase in properly binding and incorporating nucleotides.

In this report, we have further investigated the dynamics of translesion DNA synthesis by evaluating the role of divalent metal ion in the maintenance of fidelity. Although it has been demonstrated that Mn^{2+} is a potent mutagen both in vivo and in vitro (refs *17*−*19* for example), the molecular mechanism accounting for this phenomenon is poorly defined. Within this context, we asked if Mn^{2+} would enhance the rate of dNMP insertion opposite an abasic site, and if so, was this accomplished through lowering the binding energy of an incorrect dNTP and/or by enhancing the rate of conformational change preceding phosphoryl transfer? In this report, we provide kinetic evidence that substitution of Mn^{2+} for Mg^{2+} significantly enhances the rate of dNTP insertion opposite an abasic site. Furthermore, evidence is provided that Mn^{2+} changes the rate-limiting step for steady-state polymerase turnover during translesion DNA synthesis. The Mn^{2+}-induced change in the rate-limiting step is accomplished through a large enhancement in the rate of the conformational change preceding chemistry without a substantial effect on the intrinsic ground-state binding of dNTP opposite an abasic site.

MATERIALS AND METHODS

Materials

[γ-^{32}P]ATP and [α-^{32}P]dATP were purchased from New England Nuclear. Unlabeled dNTPs (ultrapure) were obtained from Pharmacia. $MgCl_2$, $MnCl_2$, and all buffers were from Sigma. All other materials were obtained from commercial sources and were of the highest available quality. Oligonucleotides, including those containing a tetrahydrofuran moiety mimicking an abasic site, were synthesized by Operon Technologies (Alameda, CA). Single-stranded and duplex DNA were purified and quantified as previously described (*20*). T4 exonuclease-deficient polymerase D129A (Asp219 to Ala mutation) was purified and quantified as previously described (*21*).

Methods

The assay buffer used in all kinetic studies consisted of 25 mM Tris-OAc (pH 7.5), 150 mM KOAc, and 10 mM 2-mercaptoethanol. All assays, including rapid quench experiments using the instrument described by Johnson (*22*), were performed at 25 °C. Polymerization reactions were monitored by analysis of the products on 20% sequencing gels as described by Mizrahi et al. (*23*). Gel images were obtained with a Molecular Dynamics PhosphorImager. Product formation was quantified by measuring the ratio of ^{32}P-labeled extended to nonextended primer. The ratios of product formation are corrected for substrate in the absence of polymerase (zero point). Corrected ratios are then multiplied by the concentration of the primer−template species used in each assay to yield total product.

Steady-State Incorporation Assays. Steady-state rates of dNTP incorporation across from the abasic site were measured as previously described (*11*). Briefly, initial rates of primer extension were measured using a fixed amount of T4 exo$^-$ polymerase (50 nM), DNA substrate (1000 nM), and metal ion (10 mM $MnCl_2$ or 10 mM $MgCl_2$) at various concentrations of dNTP (0.01−5 mM). Aliquots of the reaction were quenched into EDTA (0.5 M, pH 7.4) at times ranging from 5 to 600 s. Samples were diluted 1:1 with sequencing gel load buffer, and products were analyzed for product formation by denaturing gel electrophoresis. In all

13/20$_T$-MER

```
5′-TCGCAGCCGTCCA
3′-AGCGTCGGCAGGTTCCCAAA
```

13/20SP-MER

```
5′-TCGCAGCCGTCCA
3′-AGCGTCGGCAGGTSpCCCAAA
```

FIGURE 1: DNA substrates used for kinetic analysis. Sp denotes the tetrahydrofuran moiety designed to mimic an abasic site.

cases, steady-state rates were obtained from the linear portion of the time course. Data obtained for steady-state rates in DNA polymerization measured under pseudo-first-order reaction conditions were fit to eq 1

$$y = mt + b \quad (1)$$

where m is the slope of the line, b is the y-intercept, and t is time.

Pre-Steady-State Nucleotide Incorporation Assays. Time courses of dNTP incorporation were examined using either 13/20$_T$-mer or 13/20SP-mer (Figure 1) using a rapid quench instrument (*22*). A preincubated solution of 200 nM T4 exo$^-$ polymerase, 1000 nM 5′-labeled DNA, and 100 μM EDTA was mixed with an equal volume of a solution containing 20 mM $MnCl_2$ and variable concentrations of dNTP in the same reaction buffer. The reaction was then terminated at various times by adding 500 mM EDTA. Polymerization products were analyzed as described above. Data were fit to eq 2 which defines a burst in product formation followed by a steady-state rate

$$y = Ae^{-kt} + Bt + C \quad (2)$$

where A is the burst amplitude, k is the first-order rate constant, B is the steady-state rate, t is time, and C is the apparent burst amplitude determined from extrapolation of the steady-state phase to time zero.

Single-Turnover Nucleotide Incorporation Assays. T4 exo$^-$ polymerase (300 nM) was incubated with 150 nM DNA (13/20SP-mer) in assay buffer containing 100 μM EDTA and mixed with variable concentrations of dNTP (0.01−4 mM) and 20 mM $MnCl_2$. The reactions were quenched with 500 mM EDTA at variable times (0.005−30 s) and analyzed as described above. Data obtained for all single-turnover DNA polymerization assays were fit to eq 3

$$y = Ae^{-kt} + C \quad (3)$$

where A is the burst amplitude, k is the first-order rate constant, t is time, and C is the measured end point in product formation. Data for the dependency of k_{obs} as a function of dNTP concentration were fit to the Michaelis−Menten equation

$$k_{obs} = k_{pol}[\text{dNTP}]/K_d + [\text{dNTP}] \quad (4)$$

where k_{obs} is the observed first-order rate constant, k_{pol} is the rate of DNA polymerization, K_d is the equilibrium dissociation constant for dNTP, and [dNTP] is the concentration of nucleotide substrate.

RESULTS AND DISCUSSION

Manganese Enhances the Overall Efficiency of Translesion DNA Synthesis. The effect of substituting Mn^{2+} for Mg^{2+} on the efficiency of nucleotide incorporation across from an abasic site was evaluated using the 13/20SP-mer DNA substrate (Figure 1). Rates were monitored through the addition of each dNTP singly to a preincubated solution of 50 nM T4 exo$^-$ with 1000 nM 5′-labeled 13/20SP-mer in the presence of either divalent metal (10 mM). To compare the effect of metal ion substitution, the concentration of dNTP was maintained fixed at its respective K_m value previously reported using Mg^{2+} (*11*). Representative data presented in Figure 2A clearly show an enhancement in the rate of dAMP insertion in the presence of Mn^{2+} as opposed to Mg^{2+}. This enhancement is not limited to dAMP insertion since the rates of incorporation for each dNTP were 11−34-fold faster when Mn^{2+} was substituted for Mg^{2+} (Table 1).

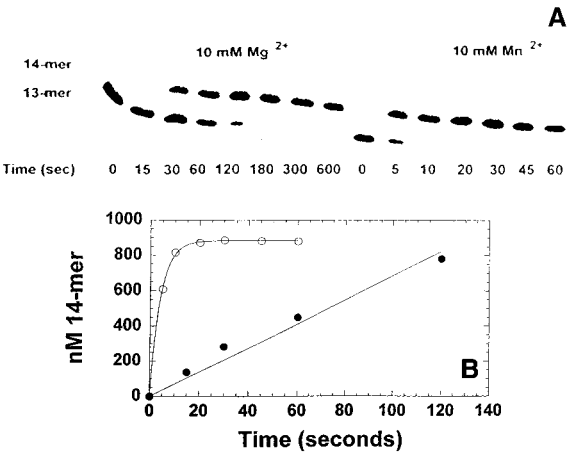

FIGURE 2: Manganese enhances the rate of dAMP insertion opposite an abasic site. (A) Representative data for the insertion of dAMP opposite an abasic site in the presence of either Mg^{2+} or Mn^{2+}. (B) Time course for dAMP insertion opposite an abasic site in the presence of either Mg^{2+} (●) or Mn^{2+} (○).

Table 1: Summary of Initial Velocity Rates for dNTP Incorporation Opposite an Abasic Site or T in the Presence of Mn^{2+} or Mg^{2+} [a]

	13/20SP-mer			13/20$_T$-mer		
	rate (nM/s)		fold	rate (nM/s)		fold
dNTP	Mn^{2+}	Mg^{2+}	increase[b]	Mn^{2+}	Mg^{2+}	increase
dATP	~100	8.3 ± 0.7	12	>100	>100	ND[c]
dCTP	1.7 ± 0.3	0.05 ± 0.01	34	5.9 ± 0.8	0.9 ± 0.11	7
dGTP	11.1 ± 0.7	0.64 ± 0.09	17	2.9 ± 0.7	0.30 ± 0.05	10
dTTP	12.8 ± 0.9	1.21 ± 0.11	11	11.3 ± 0.7	0.83 ± 0.09	14

[a] Rates were monitored through the addition of each dNTP singly to a preincubated solution of 50 nM T4 exo$^-$ with 1000 nM 13/20SP-mer or 13/20$_T$-mer in the presence of either 10 mM Mg^{2+} or 10 mM Mn^{2+}. The concentration of dNTP was fixed as follows: 50 μM dATP, 1 mM dCTP, 150 μM dGTP, and 700 μM dTTP. [b] Refers to the fold enhancement in replication efficiency when Mn^{2+} is substituted for Mg^{2+}. [c] No difference detected under these conditions.

Similar steady-state analysis was performed using the 13/20$_T$-mer DNA substrate (Figure 1) to evaluate the effect of Mn^{2+} on the kinetics of misincorporation. As presented in Table 1, the rates of dNTP misincorporation opposite T are also enhanced in the presence of Mn^{2+}. In general, the magnitude of the rate enhancement for misincorporation (7−14-fold) is similar to that observed for misinsertion opposite the abasic site (11−34-fold).

Change in the Rate-Limiting Step during dAMP Insertion Opposite an Abasic Site. As depicted in Figure 2B, the time course of dAMP insertion across from the abasic site in the presence of Mg^{2+} is linear. During nucleotide insertion

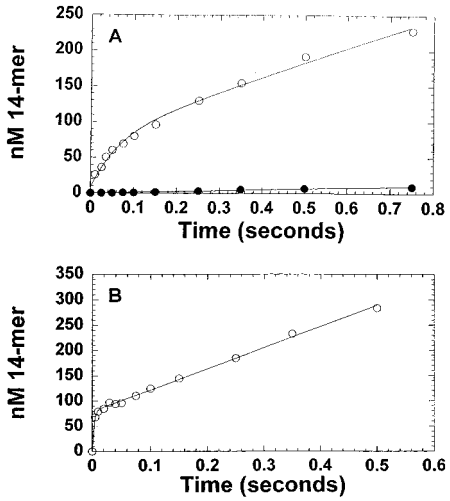

FIGURE 3: (A) Pre-steady-state time course of dAMP insertion using 13/20SP-mer in the presence of Mn^{2+} (○) or Mg^{2+} (●). Assays were performed by mixing a preincubated solution of 200 nM T4 exo$^-$ polymerase and 1000 nM 5′-labeled 13/20SP-mer with an equal volume of a solution containing 20 mM Mn^{2+} and 200 μM dATP or 20 mM Mg^{2+} and 200 μM dATP in the same reaction buffer using a rapid quench instrument (*22*). The reaction was terminated at the various times denoted by adding 500 mM EDTA. The solid line for the time course was obtained by fitting the data to the kinetic model depicted in Scheme 1 in which the rate-limiting step for enzyme turnover is the release of polymerase from extended DNA (step 7). (B) Pre-steady-state time course of dAMP insertion using 13/20T-mer in the presence of Mn^{2+}. Assays were performed by mixing a preincubated solution of 200 nM T4 exo$^-$ polymerase and 1000 nM 5′-labeled 13/20T-mer with an equal volume of a solution containing 20 mM Mn^{2+} and 200 μM dATP in the same reaction buffer using a rapid quench instrument (*22*). The reaction was terminated at the various times denoted by adding 500 mM EDTA. The solid line for the time course was obtained by fitting the data to the kinetic model depicted in Scheme 1 in which the rate-limiting step for enzyme turnover is the release of polymerase from extended DNA (step 7).

opposite an abasic site, this linear time course indicates that the rate-limiting step for enzyme turnover is the conformational change preceding chemistry (*11*). Perhaps the most surprising effect of Mn^{2+} is the observation of an apparent burst in dAMP insertion across from the abasic site (Figure 2B). This apparent burst suggests that the conformational change preceding chemistry is no longer rate-limiting for enzyme turnover. To further evaluate the dynamics of this process, the kinetics of dAMP insertion opposite the abasic site were monitored on a millisecond time scale ($\Delta t = 10-750$ ms) using a rapid quench instrument (*22*). The time course obtained under pseudo-first-order reaction conditions using Mn^{2+} is biphasic (Figure 3A), characterized by a rapid initial burst in product equivalent to the concentration of enzyme followed by a second, slower phase in product formation representing product release and subsequent utilization of the remaining substrate. The time course was fit to the equation for a single exponential followed by a steady-state phase (eq 2), yielding a k_{obs} of 14.9 ± 4.1 s^{-1} and a k_{cat} of 2.4 ± 0.3 s^{-1} (obtained by dividing the steady-state rate by the burst amplitude).

The insertion of dAMP opposite T was assessed in the presence of Mn^{2+} to directly compare translesion DNA synthesis with precise DNA replication. As anticipated, the time course displayed an initial burst in DNA_{n+1} production followed by a second, slower phase in DNA_{n+1} formation

Table 2: Kinetic Constants for dATP Incorporation Catalyzed by T4 Exo$^-$ DNA Polymerase

dNTP	DNA substrate	k_{obs} (s^{-1})	k_{cat} (s^{-1})
dATP[a]	13/20$_T$-mer (Mg^{2+})	160 ± 30	2.3 ± 0.2
dATP[a]	13/20$_T$-mer (Mn^{2+})	180 ± 25	2.3 ± 0.2
dATP[b]	13/20SP-mer (Mg^{2+})	ND[c]	0.12 ± 0.03
dATP[d]	13/20SP-mer (Mn^{2+})	14.9 ± 4.1	2.4 ± 0.3

[a] Correct incorporation of dATP across from T was assessed under pseudo-first-order reaction conditions using 100 nM T4 exo$^-$, 500 nM 13/20$_T$-mer, and 100 μM dATP in the presence of either 10 mM Mg^{2+} or 10 mM Mn^{2+}. [b] Data previously reported by Berdis (*11*). Briefly, incorporation of dATP across from an abasic site was assessed using 100 nM T4 exo$^-$, 500 nM 13/20SP-mer, and 100 μM dATP in the presence of 10 mM Mg^{2+}. [c] No burst detected. [d] Incorporation of dATP across from an abasic site was assessed using 100 nM T4 exo$^-$, 500 nM 13/20SP-mer, and 50 μM dATP in the presence of 10 mM Mn^{2+}.

(Figure 3B). The k_{obs} value of 160 ± 30 s^{-1} measured in the presence of Mn^{2+} is identical, within experimental error, to the rate constant of 180 ± 25 s^{-1} measured using Mg^{2+} (data not shown). During precise replication, the release of polymerase from extended DNA (DNA_{n+1}) also appears to be insensitive to metal ion since a k_{cat} value of 2.3 ± 0.2 s^{-1} is obtained in either case and is identical to previously published values (*20, 21*). Values for k_{obs} and k_{cat} during precise and translesion DNA synthesis in the presence of either Mn^{2+} or Mg^{2+} are summarized in Table 2.

Single-turnover experiments were then performed to measure the maximal polymerization rate constant, k_{pol}, across from the abasic site. In these experiments, the kinetics of dAMP insertion were monitored on a millisecond time scale ($\Delta t = 5-5000$ ms) by rapidly mixing a preincubated solution of T4 exo$^-$ polymerase (300 nM) and 5′-labeled 13/20SP-mer (150 nM) with an equal volume of a solution containing 10 mM $MnCl_2$ and variable concentrations of dATP (10−1000 μM). All time courses of primer extension were best defined as a single-exponential process (Figure 4A) and fit to eq 3. As shown in Figure 4B, the plot of k_{obs} versus dATP concentration is hyperbolic, yielding a k_{pol} of 40 ± 3 s^{-1} and a K_d of 150 ± 25 μM. Values for k_{pol}, K_d, and k_{pol}/K_d using dATP are summarized in Table 3.

The elemental effect on the kinetics of dAMP insertion was then measured employing single-turnover conditions using either 50 μM α-S-dATP or α-O-dATP (concentrations that were lower than K_d). In each case, the time course of DNA_{n+1} production was fit to a single exponential to yield k_{obs} values of 3.5 ± 0.3 and 8.5 ± 0.9 s^{-1} with α-S-dATP and α-O-dATP, respectively (data not shown). Although substitution of α-S-dATP for α-O-dATP slows the rate of polymerization by 2.4-fold, this relatively low elemental effect suggests that phosphoryl transfer does not limit dAMP incorporation across from the abasic site.[2]

On the basis of the biphasic time course as well as the near identity in the k_{cat} values obtained in the presence of Mn^{2+} or during precise DNA replication (vida supra; *20, 21*), we denote the rate-limiting step for steady-state enzyme turnover as the release of enzyme from product DNA. The change in the rate-limiting step directly contrasts the dynamics of translesion DNA synthesis using Mg^{2+} as the divalent metal ion in which the conformational change preceding chemistry is completely rate-limiting for enzyme turnover (*11*). Direct comparison of the rate constants in primer elongation (k_{pol}) across from the abasic site reveals an ~270-

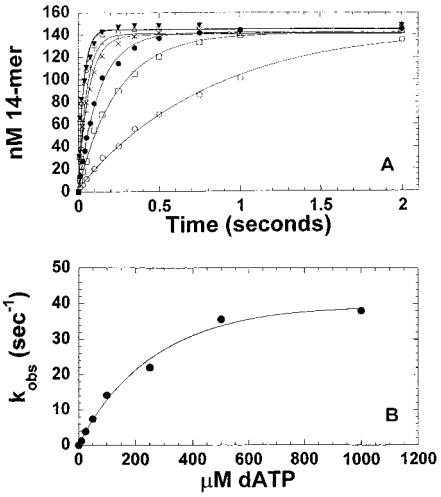

FIGURE 4: dATP concentration dependence on the apparent burst rate under single-turnover conditions. (A) T4 exo$^-$ polymerase (300 nM) and 5′-labeled 13/20SP-mer (150 nM) were preincubated and mixed with increasing concentrations of Mn^{2+} and dATP to initiate the reaction, and the reaction was quenched with 500 mM EDTA at variable times (0.01−2 s). The incorporation of dATP was analyzed by denaturing gel electrophoresis. The dATP concentrations were 10 (○), 25 (□), 50 (●), 100 (×), 250 (+), 500 (△), and 1000 μM (▼). The solid lines represent the fit of the data to a single exponential. (B) The observed rate constants for dATP incorporation (●) were plotted against dATP concentration and fit to a hyperbola to determine values corresponding to K_d and k_{pol}.

Table 3: Kinetic Rate and Equilibrium Constants for dNTP Incorporation Opposite an Abasic Site in the Presence of Mn^{2+} [a]

dNTP	k_{pol} (s^{-1})	K_d (μM)	k_{pol}/K_d (M^{-1} s^{-1})
dATP	40 ± 3	165 ± 25	2.42×10^5
	(0.15 ± 0.01)[b]	(35 ± 5)	(4.3×10^3)
dCTP	0.62 ± 0.08	750 ± 75	830 (32)
	(0.008 ± 0.001)	(250 ± 50)	
dGTP	1.4 ± 0.1	50 ± 5	2.8×10^4
	(0.023 ± 0.005)	(130 ± 20)	(180)
dTTP	0.72 ± 0.11	165 ± 15	4.2×10^3
	(0.055 ± 0.011)	(1200 ± 200)	(46)

[a] Assays performed under single-turnover conditions used 300 nM T4 exo$^-$ DNA polymerase, 150 nM 13/20SP-mer, and variable concentrations of dNTP in the presence of 10 mM $MnCl_2$. [b] Values in parentheses are those previously published using Mg^{2+} as the divalent metal ion (*11*) and are provided for comparison.

fold enhancement in the rate of the conformational change preceding chemistry induced by Mn^{2+} [compare the value of 0.15 s^{-1} obtained using Mg^{2+} (*11*) with the value of 40 s^{-1} obtained using Mn^{2+}]. Surprisingly, although the rate of the conformational change is enhanced, the level of binding of dATP to the polymerase−DNA complex actually decreases 3-fold [compare the value of 50 μM reported with Mg^{2+} (*11*) to the value of 165 μM obtained using Mn^{2+}].

Phosphoryl Transfer Is Rate-Limiting for the Incorporation of dCTP, dGTP, and dTTP. Substitution of Mn^{2+} for Mg^{2+} also enhances the rate of dCMP, dGMP, and dTMP misinsertion opposite the abasic site. We further evaluated the dynamics of this process by monitoring the kinetics of their insertion opposite an abasic site on the millisecond time scale. Time courses were generated in the presence of Mn^{2+}, using either 1 mM dCTP or 1 mM dTTP while the concentration of dGTP was maintained at 150 μM.[3] All time courses were linear and devoid of a measurable burst in DNA_{n+1} production (Figure 5). These linear time courses are distinctively different from that obtained with dATP and suggest that either phosphoryl transfer or a kinetic step preceding phosphoryl transfer is rate-limiting for enzyme turnover with these dNTPs. A fit of each data set to the equation for a straight line (eq 1) yielded steady-state rates of 12, 120, and 64 nM/s for the insertion of dCMP, dGMP, and dTMP, respectively.

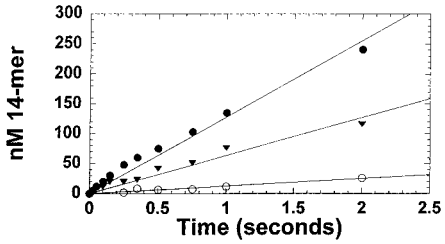

FIGURE 5: Pre-steady-state time course of dCMP (○), dGMP (●), or dTMP (▼) insertion opposite an abasic site using Mn^{2+} as the divalent metal ion. Assays were performed by rapidly mixing a preincubated solution of 200 nM T4 exo$^-$ polymerase and 1000 nM 5′-labeled 13/20SP-mer with an equal volume of a solution containing 20 mM Mn^{2+} with 300 μM dGTP or 2 mM dCTP or dTTP in the same reaction buffer. The reaction was terminated at times varying from 0.01 to 2 s by adding 500 mM EDTA. The solid lines for each time course were obtained by fitting the data to the kinetic model depicted in Scheme 1 in which the rate-limiting step for enzyme turnover is phosphoryl transfer (step 4).

Single-turnover experiments were then performed by varying the concentration of dCTP or dTTP from 0.01 to 2.5 mM (data not shown) to measure the maximal polymerization rate constant for insertion opposite an abasic site. Insertion opposite the abasic site was observed at all dNTP concentrations that were employed, and the time courses were fit to the equation describing a single-exponential process to yield values reflecting k_{obs}. The plots of k_{obs} versus dCTP or dTTP concentration were hyperbolic (data not shown). A k_{pol} value of 0.62 ± 0.8 s^{-1} and a K_d value of 750 ± 75 μM were measured with dCTP. Using dTTP, the k_{pol} value was 0.72 ± 0.11 s^{-1} while the K_d value was 165 ± 15 μM. Values for k_{pol}, K_d, and k_{pol}/K_d are summarized in Table 3.

The elemental effect on the kinetics of dCMP insertion opposite the abasic site was measured under single-turnover

[2] There has been much debate regarding the utility of thio elemental effects as a quantitative assessment of which kinetic step is rate-limiting for catalysis (*24*−*27*). For example, using the Klenow fragment as the DNA polymerase, Mizrahi et al. (*24*) originally observed a small elemental effect of 1.6 in the direction of polymerization and a relatively large effect of 18 in the direction of pyrophosphorolysis. This difference was partially attributed to the increase in K_{eq} upon replacement of α-O-dNTP with α-S-dNTP (*24*). Likewise, substitution of α-O-dNTP with α-S-dNTP can affect the secondary structure of nucleic acid (*25*), which can lead to perturbations in processes other than phosphoryl transfer. It should be noted that in our study, the relative magnitude of the measured elemental effects is being utilized as preliminary evidence for whether phosphoryl transfer is the rate-limiting step for insertion of a dNMP opposite an abasic site. Further experimentation is clearly required to fully evaluate if the measured elemental effect reflects events associated solely with chemistry or other physical processes involving protein and/or nucleic acid.

[3] In the presence of Mn^{2+}, substrate inhibition at high dGTP concentrations (>750 μM) was observed. Thus, the concentration of dGTP was maintained at 150 μM to evaluate the presence of a burst in dGMP insertion. If a step after phosphoryl transfer were rate-limiting, a burst in initial product formation would be observed even at K_m levels of dGTP. However, the rate of the burst phase would be slower than if saturating ($10K_m$) dGTP concentrations were maintained.

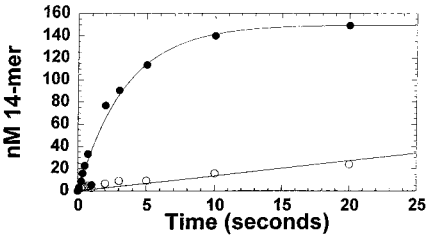

FIGURE 6: Elemental effect on dCMP insertion opposite an abasic site in the presence of Mn^{2+}. Assays were performed by rapidly mixing a preincubated solution of 200 nM T4 exo$^-$ polymerase and 1000 nM 5′-labeled 13/20SP-mer with an equal volume of a solution containing 20 mM Mn^{2+} with either 2 mM α-O-dCTP (●) or 2 mM α-S-dCTP (○) in the same reaction buffer. The reaction was terminated at times varying from 0.01 to 20 s by adding 500 mM EDTA. The solid lines for each time course were obtained by fitting the data to the kinetic model depicted in Scheme 1 in which the rate-limiting step for enzyme turnover is phosphoryl transfer (step 4).

Scheme 1: Kinetic Mechanism for the Bacteriophage T4 DNA Polymerase

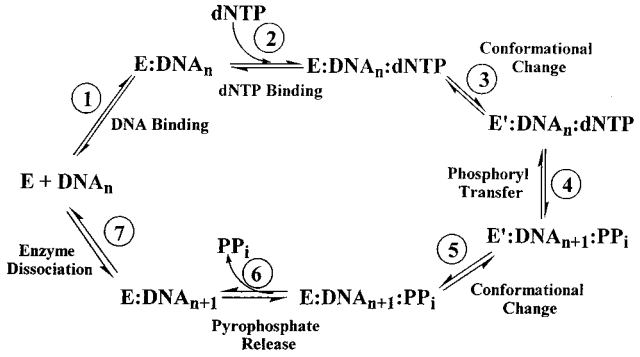

conditions. Using 1 mM α-S-dCTP, the time course of DNA_{n+1} production was linear under the time frame that was examined (0.025−20 s) and directly contrasts the single-exponential time course obtained using 1 mM α-O-dCTP (Figure 6). Computer simulation using KinSim (*28*) was performed as previously described (*11*) to obtain individual rate constants for either time course. Each time course was fit to the minimal kinetic scheme depicted in Scheme 1 to provide k_{obs} values of 0.35 ± 0.03 s^{-1} using α-O-dCTP and 0.013 ± 0.004 s^{-1} using α-S-dCTP. The ratio of the rate constants, k^o/k^s, reveals a significant elemental effect of ∼27, thus suggesting that phosphoryl transfer is at least partially rate-limiting for dCMP insertion opposite the abasic site.

Single-turnover experiments were likewise performed by varying the concentration of dGTP from 0.01 to 2.5 mM. Extension opposite and beyond the abasic site was observed at all dGTP concentrations that were tested since dGTP is the correct triphosphate for the next three incorporations (data not shown). However, the reaction kinetics were simplified by assessing only the depletion of the 13-mer substrate as a function of time. Surprisingly, the rate of 13-mer depletion in the presence of Mn^{2+} was retarded using dGTP concentrations of >750 μM. Although the reason for this apparent substrate-induced inhibition is currently unknown, the plot of k_{obs} versus dGTP concentrations ranging from 10 to 750 μM (data not shown) is hyperbolic, yielding a k_{pol} of 1.4 ± 0.1 s^{-1} and a K_d of 50 ± 5 μM. Values for k_{pol}, K_d, and k_{pol}/K_d using dGTP are summarized in Table 3.

Under single-turnover conditions, utilization of 500 μM α-S-dGTP yields a rate constant of 0.02 s^{-1} for insertion

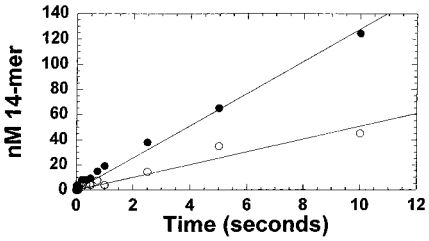

FIGURE 7: Pre-steady-state time course of dCMP misincorporation opposite T using Mn^{2+} as the divalent metal ion. Assays were performed by rapidly mixing a preincubated solution of 150 nM T4 exo$^-$ polymerase and 1000 nM 5′-labeled 13/20T-mer with an equal volume of a solution containing 20 mM Mn^{2+} with either 2 mM α-O-dCTP (●) or 2 mM α-S-dCTP (○) in the same reaction buffer. The reaction was terminated at times varying from 0.01 to 10 s by adding 500 mM EDTA. The solid lines for each time course were obtained by fitting the data to the kinetic model depicted in Scheme 1 in which the rate-limiting step for enzyme turnover is the conformational change preceding phosphoryl transfer (step 3).

across from the abasic site (data not shown). When compared to the rate constant of 1.4 s^{-1} directly measured for the insertion of 500 μM α-O-dGTP, the large elemental effect of 70 argues that phosphoryl transfer is the rate-limiting step for the insertion of dGMP across from the abasic site. It should be noted that the large elemental effect of 70 observed in the presence of Mn^{2+} directly contrasts the relatively low value of 3.1 previously reported with Mg^{2+} as the metal cofactor (*11*).

Effect of Mn^{2+} on the Mechanism of dCTP Misincorporation Opposite T. As discussed earlier, substitution of Mn^{2+} for Mg^{2+} also enhances the efficiency of misincorporation of dCTP, dGTP, and dTTP opposite T. To further evaluate the dynamics of misincorporation induced by Mn^{2+}, the time course of dCMP misinsertion opposite T was measured on a millisecond time scale. Under pseudo-first-order reaction conditions, the time course of misincorporation is linear (Figure 7). Since a saturating concentration of dCTP (2 mM) was employed, a k_{cat} value of 0.17 ± 0.03 s^{-1} was obtained by dividing the steady-state rate by the active enzyme concentration. When the reaction is monitored under single-turnover conditions, the resulting time course is best defined by a single-exponential process (data not shown), yielding a k_{obs} value of 0.18 ± 0.01 s^{-1}, essentially identical to the rate constant obtained under pseudo-first-order reaction conditions. The identity in rate constants coupled with the lack of a detectable burst in primer extension indicates that the insertion of dCMP opposite T, even in the presence of Mn^{2+}, is limited by the conformational change preceding phosphoryl transfer. Furthermore, utilization of α-S-dCTP under pseudo-first-order (Figure 7) and single-turnover reaction conditions (data not shown) yields low elemental effects of 2.8 and 2.4, respectively, suggesting that phosphoryl transfer is not rate-limiting for dCTP misincorporation in the presence of Mn^{2+}. Collectively, these data indicate that the dynamics of dCTP misincorporation differ substantially from those of dCMP misinsertion opposite an abasic site.

Conclusions. The fidelity of DNA replication is accomplished through a multistep pathway catalyzed by the DNA polymerase. Arguably, the most important kinetic step in this pathway is the conformational change step that is flanked by kinetic steps involving initial dNTP binding and phosphoryl transfer (Scheme 1, steps 2−4). We have

previously evaluated the importance of the conformational change preceding phosphoryl transfer within the context of translesion DNA synthesis (*11*). Using Mg^{2+} as the divalent metal ion, this kinetic step is the rate-limiting step for polymerase turnover during dNMP insertion opposite an abasic site (*11*). The kinetic data described in this report clearly indicate that substitution of Mn^{2+} for Mg^{2+} greatly enhances the rate of dNMP insertion opposite an abasic DNA lesion. This rate enhancement is caused primarily by a metal-ion induced change in the rate-limiting step for polymerase turnover during translesion DNA synthesis. This is most evident in the case of dAMP insertion in which, under pseudo-first-order reaction conditions, the biphasic time course of primer elongation indicates that a step after phosphoryl transfer is rate-limiting for enzyme turnover. We have denoted this step as the release of polymerase from extended DNA (Scheme 1, step 7). However, it should be emphasized that the rate-limiting step for dAMP insertion opposite the abasic site is the conformational change preceding chemistry (Scheme 1, step 3). Consistent with this argument is the fact that the k_{pol} value of 40 s^{-1} measured under single-turnover conditions is 20-fold greater than the measured k_{cat} value of ~2 s^{-1}. Furthermore, the lack of a significant elemental effect in dAMP insertion indicates that phosphoryl transfer is not rate-limiting for insertion opposite the abasic site. Thus, the k_{pol} value of 40 s^{-1} reflects the rate of the conformational change preceding the chemical event, indicating that Mn^{2+} enhances the rate of this kinetic step 270-fold [compare a value of 40 s^{-1} with Mn^{2+} vs a value of 0.15 s^{-1} with Mg^{2+} (*11*)].

As was the case using Mg^{2+} as the divalent metal ion, the dynamics of insertion opposite an abasic site are still dNTP-dependent in the presence of Mn^{2+}. This is best exemplified by the qualitative change in the time course for dNMP insertion as a function of dNTP. For example, under pseudo-first-order conditions, a biphasic time course of primer elongation is obtained with dATP while linear time courses were observed for the insertion of dCMP, dGMP, and dTMP opposite the abasic site under nearly identical reaction conditions. The linear time course is consistent with the conformational change preceding phosphoryl transfer being the rate-limiting step for polymerase turnover as previously demonstrated (*11*). However, the significant elemental effects of ~27 and ~70 measured for the insertion of dCMP and dGMP, respectively, argue that phosphoryl transfer is predominantly rate-limiting for the incorporation of these nucleoside triphosphates. By inference, the rate of the conformational change preceding phosphoryl transfer must be faster or at least as fast as the chemistry step. If correct, then the k_{pol} values of ~1 s^{-1} measured for the insertion of dCMP, dGMP, and dTMP reflect the rate constant for phosphoryl transfer, and represent a 10^3-fold reduction when compared to the rate constant assigned during precise DNA polymerization (*20*).

It is important to note that Mn^{2+} does not alter the rate-limiting step in enzyme turnover for typical misincorporation events. This is evident in the case of dCMP misincorporation opposite T in which the rate of misinsertion is at least 7-fold faster with Mn^{2+} than with Mg^{2+}. However, the linear time course of primer elongation coupled with a low elemental effect (ca. 2.8) suggests that Mn^{2+}-induced misincorporation is solely limited by the conformational change preceding phosphoryl transfer as is the case using Mg^{2+} (*11*). Thus, the dynamics by which the T4 DNA polymerase performs misinsertion and misincorporation differ substantially.

Although Mn^{2+} enhances the rate of misincorporation and misinsertion, the molecular mechanism accounting for this phenomenon remains elusive. The kinetic data presented here clearly indicate that during translesion DNA synthesis, the rate of the conformational change preceding phosphoryl transfer is affected by Mn^{2+}. During DNA polymerization, this conformational change is viewed as the kinetic step in which the DNA polymerase places the incoming dNTP into the proper geometric arrangement for phosphoryl transfer to occur (*12*). The underlying implication is that this kinetic step reflects formation of hydrogen bonds between the incoming dNTP and template nucleobase. It is intuitively obvious that the lack of potential hydrogen bonds at an abasic site should slow the rate of conformational change since binding of any dNTP presumably results in an inappropriate fit in the enzyme's active site. While the slow rates measured for the conformational change using Mg^{2+} as the divalent metal ion are consistent with this model (*11*), the ability of Mn^{2+} to significantly accelerate the conformational change preceding phosphoryl transfer at this type of lesion is intriguing.

A thermodynamic analysis was performed using the kinetic rate and equilibrium constants provided in Table 3 to evaluate the relative free energy change ($\Delta\Delta G°$) associated with the metal ion-induced enhancement in translesion DNA synthesis.[4] Direct comparison of k_{pol}/K_d values for dAMP insertion using either Mg^{2+} or Mn^{2+} reveals an overall decrease in $\Delta\Delta G°$ of ~2.9 kcal/mol.[5] This value reflects the overall efficiency of translesion DNA synthesis and is composed of two kinetically distinct components, one intimately associated with ground-state binding and the other associated with the conformational change preceding chemistry. On the basis of differences in the K_d for dATP, the $\Delta\Delta G°$ for ground-state binding is roughly 0.65 kcal/mol higher in the presence of Mn^{2+} [compare a value of 35 μM with Mg^{2+} (*11*) vs a value of 165 μM with Mn^{2+}]. Thus, initial binding of dATP is actually disfavored in the presence of Mn^{2+}. However, the faster rate of conformational change induced by Mn^{2+} corresponds to a substantial lowering of $\Delta\Delta G°$ of 3.31 kcal/mol [compare a value of 0.15 s^{-1} with Mg^{2+} (*11*) vs a value of 40 s^{-1} with Mn^{2+}]. Surprisingly, the decrease of 3.31 kcal/mol falls within the values of ca. 0.2−4 kcal/mol associated with base pair formation (*13*−*15*).

Proper base pair formation is dependent upon both hydrogen bonding and nucleobase-stacking interactions

[4] Note that this analysis can only be performed for dAMP insertion opposite the abasic site since the conformational change is rate-limiting for nucleotide insertion using Mg^{2+} or Mn^{2+}. Our kinetic data suggest that phosphoryl transfer is rate-limiting for dCMP, dGMP, and dTMP insertion in the presence of Mn^{2+} while the conformational change is rate-limiting in the presence of Mg^{2+} (*11*). Thus, the difference in kinetic steps precludes an accurate thermodynamic comparison.

[5] $\Delta\Delta G°$ values were calculated using the equation $\Delta\Delta G° = RT \ln K$, where $R = 1.9872$ cal mol^{-1} K^{-1}, $T = 298$ K, and K is the ratio of respective kinetic equilibrium or rate constants. In this instance, the $\Delta\Delta G°$ value for the overall catalytic efficiency was calculated using the k_{pol}/K_d value of 4.3×10^3 M^{-1} s^{-1} for insertion of dAMP opposite an abasic site in the presence of Mg^{2+} (*11*) and the k_{pol}/K_d value of 2.4×10^5 M^{-1} s^{-1} for insertion of dAMP opposite an abasic site in the presence of Mn^{2+} (vida supra).

(reviewed in ref *29*). It is tempting to speculate that Mn^{2+} lowers the $\Delta\Delta G°$ for dAMP insertion by providing hydrogen bonds required for proper execution of the enzyme-mediated conformational change. Conceptually, this could be accomplished by the recruitment of additional water molecules into the active site in providing hydrogen bonding stabilization for the incoming dNTP. However, this mechanism is unlikely since it cannot account for the preferential insertion of dAMP opposite the abasic site when compared to the other dNTPs.

We previously hypothesized that during tranlesion DNA synthesis, the conformational change preceding phosphoryl transfer reflects nucleobase stacking rather than hydrogen bond formation between the incoming dNTP with the template nucleobase (*11*). This model was based upon correlating the dNTP dependency on the rate of the conformational change with NMR structures of nucleic acid containing any of the four nucleosides positioned opposite an abasic site (*16*, *30*). In these structures, dAMP is stacked in an intrahelical configuration when opposite an abasic site while dGMP exists in an inter- or extrahelical conformation (*16*, *30*). Our previous kinetic analyses using Mg^{2+} revealed that dATP and dGTP are inserted opposite the abasic site more efficiently that dCTP and dTTP, potentially by being stacked in the more energetically favorable intrahelical configuration. It is tempting to speculate that Mn^{2+} facilitates nucleobase stacking of the various dNMPs while opposite the abasic site. A formal possibility is that Mn^{2+} may enhance the rate of conformational change by stabilizing the intrahelical conformation of the nucleobase opposite the abasic site. Unfortunately, the data presented here cannot unambiguously identify the biophysical reason for such a stabilizing effect induced by Mn^{2+}. In fact, the rate enhancement in the conformational change could result from dynamic protein and/or nucleic acid movements that are completely distinct from that of the nucleoside to be inserted. We are currently employing transient fluorescent techniques in evaluating if Mn^{2+} affects the conformation of the nucleic acid, the DNA polymerase, or both.

REFERENCES

1. Miller, J. A., and Miller, E. C. (1971) *J. Natl. Cancer Inst. 47*, 5−24.
2. Holmes, G. E., Bernstein, C., and Bernstein, H. (1992) *Mutat. Res. 275*, 305−315.
3. Feig, D. L., and Loeb, L. A. (1993) *Biochemistry 32*, 4466−4473.
4. Echols, H., and Goodman, M. F. (1991) *Annu. Rev. Biochem. 60*, 477−511.
5. Lindahl, T. (1993) *Nature 362*, 709−715.
6. Krokan, H. E., Nilsen, H., Skorpen, F., Otterlei, M., and Slupphaug, G. (2000) *FEBS Lett. 476*, 73−77.
7. Moran, S., Ren, R. X., and Kool, E. T. (1997) *Proc. Natl. Acad. Sci. U.S.A. 94*, 10506−10511.
8. Hiroa, I., Ohtsuki, T., Mitsui, T., and Yokoyama, S. (2000) *J. Am. Chem. Soc. 122*, 6118−6119.
9. Matray, T. J., and Kool, E. T. (1999) *Nature 399*, 704−708.
10. McMinn, D. L., Ogawa, A. K., Wu, Y. O., Schultz, P. G., and Romesberg, F. E. (1999) *J. Am. Chem. Soc. 121*, 11585−11586.
11. Berdis, A. J. (2001) *Biochemistry 40*, 7180−7191.
12. Wong, I., Patel, S. S., and Johnson, K. A. (1991) *Biochemistry 30*, 526−537.
13. Aboul-ela, F., Koh, D., Tinoco, I. J., and Martin, F. H. (1985) *Nucleic Acids Res. 13*, 4811−4825.
14. Petruska, J., Goodman, M. F., Boosalis, M. S., Sowers, L. C., Cheong, C., and Tinoco, I. J. (1988) *Proc. Natl. Acad. Sci. U.S.A. 85*, 6252−6256.
15. Law, S. M., Eritja, R., Goodman, M. F., and Bresslauer, K. J. (1996) *Biochemistry 35*, 12329−12337.
16. Cuniasse, Ph., Fazakerley, G. V., Guschlbauer, W., Kaplan, B. E., and Sowers, L. C. (1987) *J. Mol. Biol. 213*, 303−314.
17. Sirover, M. A., and Loeb, L. A. (1976) *Proc. Natl. Acad. Sci. U.S.A. 73*, 2331−2335.
18. Chang, L. M. S., and Bollum, F. J. (1973) *J. Biol. Chem. 248*, 3398−3404.
19. Beckman, R. A., Mildvan, A. S., and Loeb, L. A. (1985) *Biochemistry 24*, 5810−5817.
20. Capson, T. L., Peliska, J. A., Kaboord, B. F., Frey, M. W., Lively, C., Dahlberg, M., and Benkovic, S. J. (1992) *Biochemistry 31*, 10984−10994.
21. Frey, M. W., Nossal, N. G., Capson, T. L., and Benkovic, S. J. (1993) *Proc. Natl. Acad. Sci. U.S.A. 90*, 2579−2583.
22. Johnson, K. A. (1995) *Methods Enzymol. 249*, 38−61.
23. Mizrahi, V., Benkovic, P. A., and Benkovic, S. J. (1986) *Proc. Natl. Acad. Sci. U.S.A. 83*, 5769−5773.
24. Mizrahi, V., Henrie, R. N., Marlier, J. F., Johnson, K. A., and Benkovic, S. J. (1985) *Biochemistry 24*, 4010−4018.
25. Eckstein, F., and Jovin, T. M. (1983) *Biochemistry 22*, 4546−4550.
26. Patel, S. S., Wong, I., and Johnson, K. A. (1991) *Biochemistry 30*, 511−525.
27. Herschlag, D., Piccirilli, J. A., and Cech, T. R. (1991) *Biochemistry 30*, 4844−4854.
28. Barshop, B. A., Wren, R. F., and Frieden, C. (1983) *Anal. Biochem. 130*, 134−145.
29. Kool, E. T. (2001) *Annu. Rev. Biophys. Biomol. Struct. 30*, 1−22.
30. Cuniasse, Ph., Sowers, L. C., Eritja, R., Kaplan, B., Goodman, M. F., Cognet, J. A. H., LeBret, M., Guschlbauer, W., and Fazakerley, G. V. (1987) *Nucleic Acids Res. 15*, 8003−8022.

BI0120648